Impact of Cooling Fluid on the Design and Performance of a Supercritical CO_2 Heat Exchanger for Applications in High-Temperature Heat Pumps

Dr. Emily Fricke (KTH Royal Institute of Technology)
Zanil Narsing (KTH Royal Institute of Technology)
Dr. Silvia Trevisan (KTH Royal Institute of Technology)
Dr. Rafael Guédez Mata (KTH Royal Institute of Technology)

The International Supercritical CO2 Energy Technologies Symposium • March 2 – 5, 2026 • Pittsburgh, PA, USA

Introduction: Motivation

- High industrial energy consumption for heating and cooling
- Potential of high-temperature heat pumps (HTHPs) with thermal energy storage (TES) for decarbonization
- CO_2 as a working fluid
- Importance of heat sink design

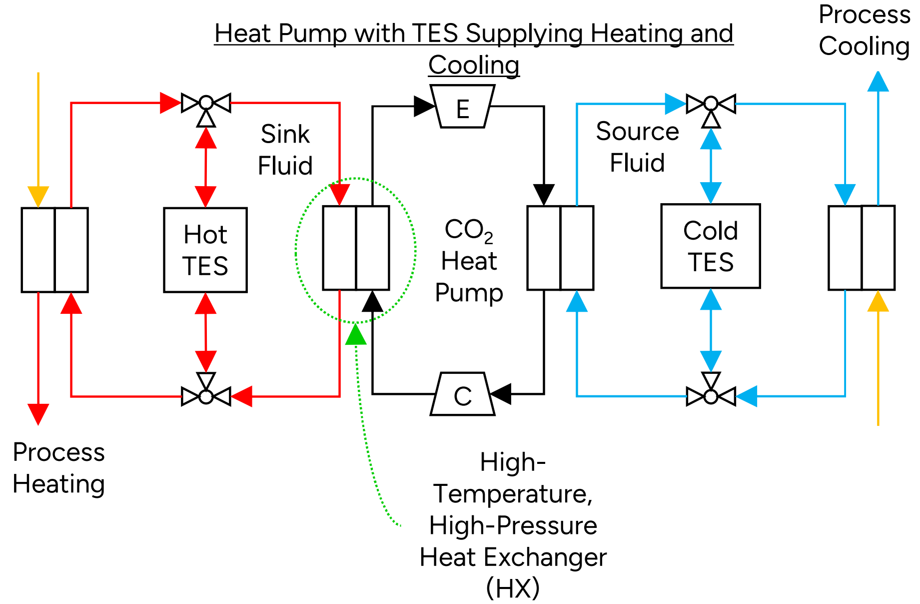

Introduction: Heat Exchanger Types

Printed Circuit Heat Exchanger (PCHE)

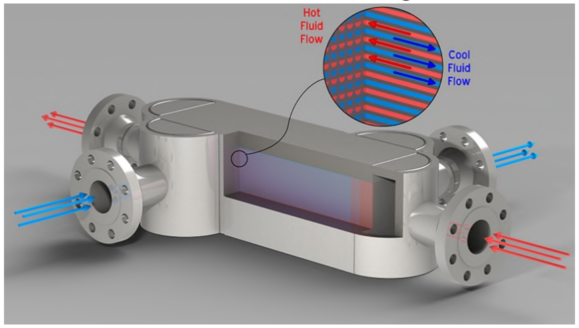

Image source: https://www.vpei.com/diffusion-bonded-microchannel-heat-exchangers/

Plate and Fin Heat Exchanger (PFHE)

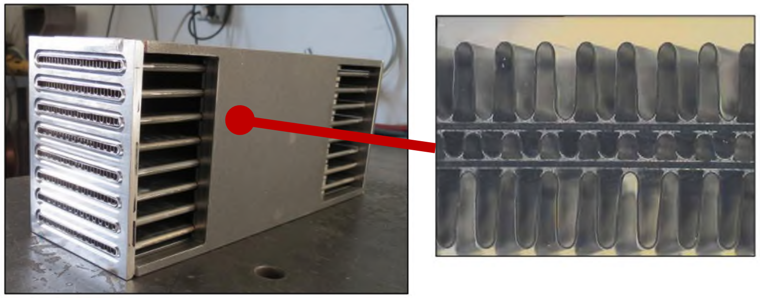

Image source: [21]

Shell and Tube Heat Exchanger (STHE)

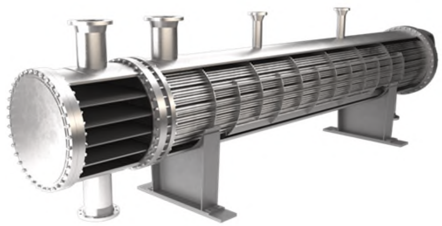

Image source: https://aager.de/ergil/heat-exchangers/

Introduction: Sink Fluids

- Thermal oil
  - \+ Suitable for high temperature, low pressure operation
  - \- Higher cost
  - \- Flammability
- Molten salt
  - \+ Suitable for high temperature, low pressure operation
  - \+ Potential to serve as TES
  - \- Higher cost
  - \- Corrosiveness
- Air
  - \+ Safe, nontoxic
  - \+ Readily available
  - \- Poor heat transfer performance

Methodology: Overview

Develop a thermofluidic model

Apply relevant boundary conditions

Vary geometric parameters to study impact on performance

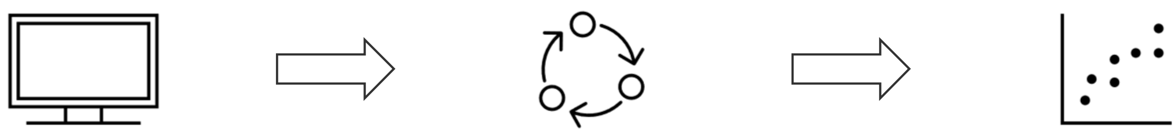

Methodology: Fluid Properties

- Oil: Duratherm 600 [7]
- MS: HITEC [9]
- Air: dry air properties from EES using equation of state developed by Lemmon et al. (2000) [10]
- CO_2: properties from EES using equation of state developed by Span and Wagner (1996) [11]

Table 1: Representative properties of fluids

Fluid	Density (kg/m^3)	Viscosity (Pa-s)	Specific Heat (J/kg-K)	Thermal Conductivity (W/m-K)
Oil (20 °C)	840	0.1002	1858	0.1405
Oil (100 °C)	787	0.0053	2114	0.136
Molten salt (200 °C)	1940	7.43e-3	1562	0.435
Air (20 °C, 5 bar)	5.953	1.827e-5	1013	0.02601
Air (100 °C, 5 bar)	4.665	2.195e-5	1015	0.03172
CO_2 (critical point: 30.98 °C, 73.77 bar)	500.6	3.493e-5	2.872e6	0.09122
CO_2 (250 °C, 200 bar)	218.9	2.956e-5	1287	0.04405

Methodology: Boundary Conditions

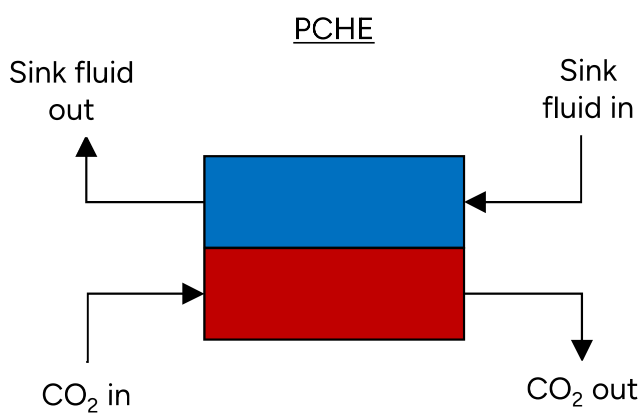

Table 3: Boundary conditions, with nominal value included in parenthesis

Fluid	Inlet Temperature (°C)	Inlet Pressure (bar)	Mass flowrate per cross-sectional area (kg/m²-s)
CO_2	250, 300 (250)	200	20
Oil	50	1	5-20 (10)
MS	150	1	10-20 (20)
Air	20	5	10-20 (20)

Methodology: PCHE Geometry

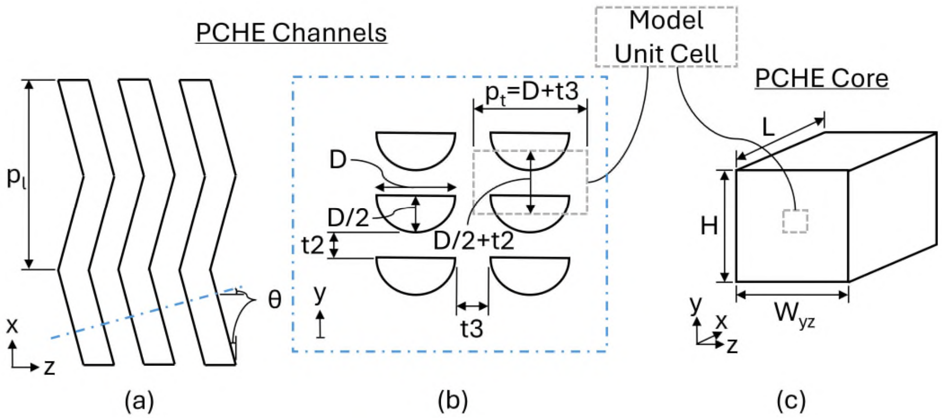

Table 4: PCHE geometric parameters, with nominal value included in bold

Parameter	Symbol	Value	Units
Diameter of semicircular channel	*D*	1.3, **1.5**, 1.7	mm
Plate thickness	*D/2+t2*	1.5	mm
Transverse pitch	p_t	1.75, **2.05**, 2.3	mm
Longitudinal pitch	p_l	8	mm
Channel angle	θ	40	°
Length	*L*	0.25-75	m

- Material: SS316L
- Cases for parametric study (CO_2 channel diameter [mm]/sink channel diameter [mm])
  - Same diameter: 1.3/1.3, 1.5/1.5, 1.7/1.7
  - Different diameter: 1.3/1.5, 1.5/1.7
- HX Length (for minimum T_{pinch}<10 °C)
  - Oil: 0.74 m
  - MS: 0.28 m
  - Air: 0.36 m

Methodology: Thermofluidic Model

Discretized Unit Cell

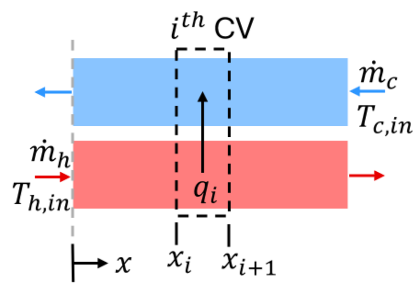

Equations

$q_i = \dot{m}(h_i - h_{i+1})$, CO_2 and air

$q_i = \dot{m}c_p(T_i - T_{i+1})$, oil and MS

$$q_i = \frac{T_{CO_2\,avg,i} - T_{sink\,avg,i}}{R_{tot,i}}$$

$$R_{tot,i} = R_{conv\,CO_2,i} + R_{cond,i} + R_{conv\,sink,i}$$

$$R_{cond,i} = \frac{t2}{k_{wall}A_{wall,i}},\ R_{conv,i} = \frac{1}{htc_i A_{conv,i}},\ htc = \frac{Nu \cdot k}{D_h}$$

$$\Delta P_i = f_i \frac{L_{channel,CV}}{2D_h} \rho_i V_i^2$$

Correlations

$Nu_{CO_2} = 0.475Re^{0.61}Pr^{0.17}$, $f_{CO_2} = 0.13Re^{-0.044}$	Saeed et al. (2020) $3000 \le Re \le 60000$ and $2.0 \le Pr \le 13$
$Nu = 4.089$, $f = \frac{15.78}{Re}$	Hesselgreaves (2001) $Re \le 2300$
$Nu = \frac{\frac{f}{8}(Re - 1000)Pr}{1 + 12.7(Pr^{2/3} - 1)\sqrt{f/8}}$	Gnielinski (1976) $2300 \le Re \le 5 \times 10^6$ and $0.5 \le Pr \le 2000$
$f = (0.790\ln(Re) - 1.64)^{-2}$	Petukhov (1970) $3000 \le Re \le 5 \times 10^6$

Results: Parametric Study, Oil

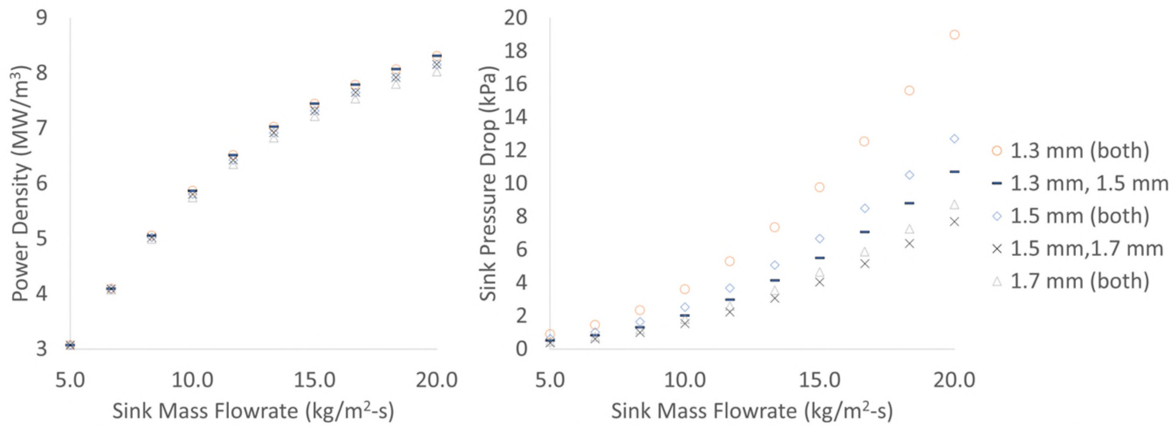

Figure 2: Parametric data for oil with a CO_2 inlet temperature of 250 °C and a heat exchanger core length of 0.74 m.

- Performance metrics
  - Power density: 3-8.3 MW/m^3
  - Sink-side pressure drop: 0.44-19.0 kPa
- Best cases
  - Highest power density: 1.3/1.5 case
  - Lowest ΔP: 1.5/1.7 case
- 1.5/1.7 => 1.3/1.5
  - 1.24% increase in power density, 35% increase in ΔP (1.26% and 35%, respectively, for 300 °C inlet temperature)

Results: Parametric Study, MS

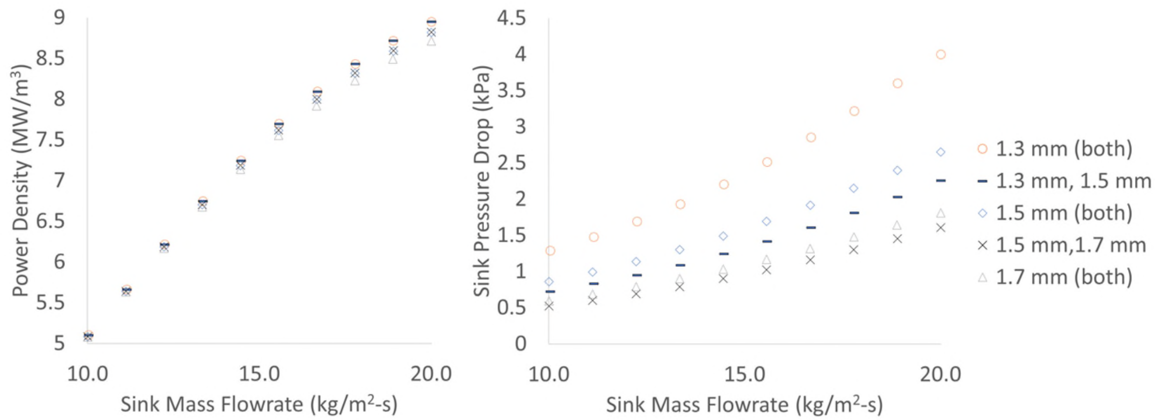

Figure 3: Parametric data for MS with a CO_2 inlet temperature of 250 °C and a heat exchanger core length of 0.28 m.

- Performance metrics
  - Power density: 5-9 MW/m^3
  - Sink-side pressure drop: 0.6-4.0 kPa
- Best cases
  - Highest power density: 1.3/1.5 case
  - Lowest ΔP: 1.5/1.7 case
- 1.5/1.7 => 1.3/1.5
  - 0.91% increase in power density, 39% increase in ΔP (0.96% and 38%, respectively, for 300 °C inlet temperature)

Results: Parametric Study, Air

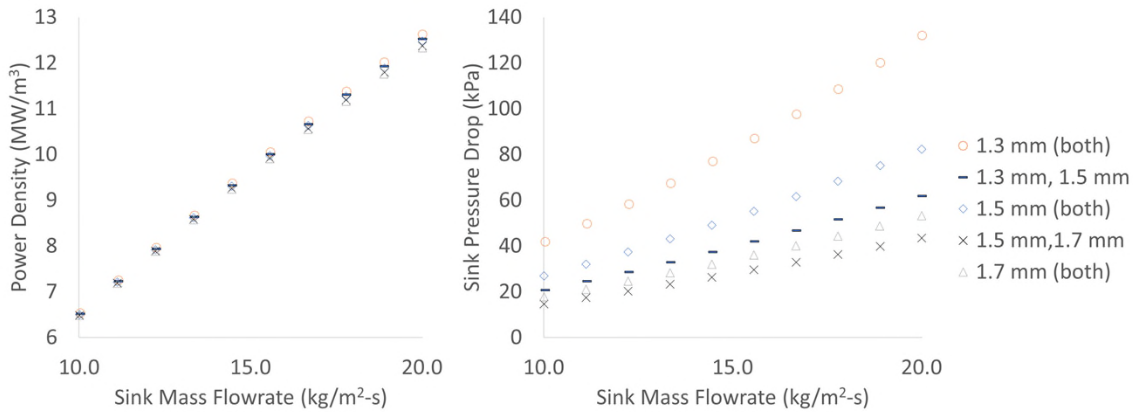

Figure 4: Parametric data for air with a CO_2 inlet temperature of 250 °C and a heat exchanger core length of 0.36 m.

- Performance metrics
  - Power density: 6.5-12.6 MW/m^3
  - Sink-side pressure drop: 14.7-132 kPa
- Best cases
  - Highest power density: 1.3/1.3 case
  - Lowest ΔP: 1.5/1.7 case
- 1.5/1.7 => 1.3/1.3
  - 1.3% increase in power density, 193% increase in ΔP (1.44% and 196%, respectively, for 300 °C inlet temperature)

Results: Parametric Study Summary

- For all fluids, 1.5/1.7 case was optimal
  - Decreasing channel size => slight increases in power density, significant increases in ΔP

Table 5: Parameters to achieve 0.5 MW HX for 250-300 °C CO_2 inlet temperature

Sink Fluid	HX Core Volume (m^3)	HX Side Length (m)	CO_2 Outlet Temperature (°C)	Pumping Power (W)
Oil	0.0686-0.0862	0.30-0.34	110-114	1.56-2.2
MS	0.0386-0.0567	0.37-0.45	161-164	1.81-3.0
Air	0.0334-0.0404	0.30-0.34	107-114	15500-16400

- Observations
  - Higher inlet temperature of MS => higher CO_2 outlet temperature
  - Lower inlet temperature of air helps enhance heat transfer
  - Pumping power ($\propto$ volumetric flowrate $\cdot$ ΔP) is very high for air case
  - => Consider lower air flowrate to achieve lower pumping power

Results: Varying HX Length

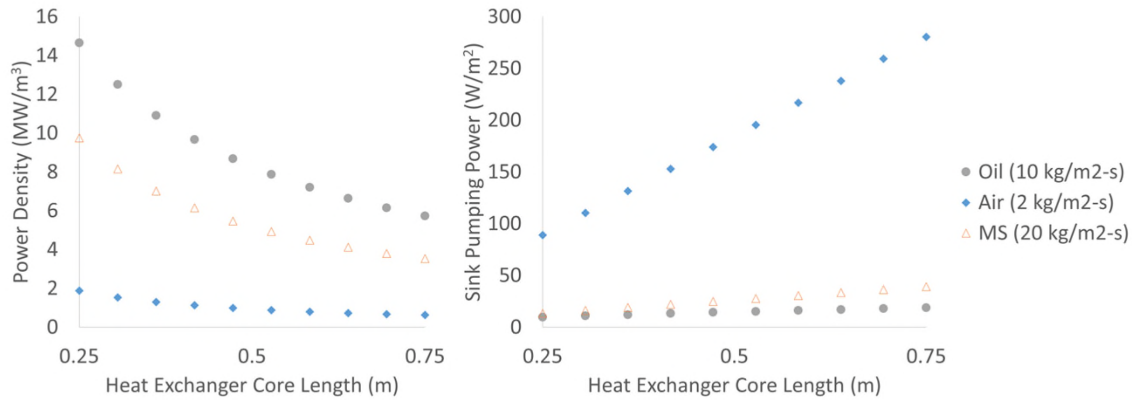

Figure 5: PCHE performance with a CO_2 inlet temperature of 250 °C for oil, MS, and air at different core lengths.

- 0.5 MW HX with air as sink (0.36 m length)
  - Volume: 0.314-0.383 m^3 (an order of magnitude larger than oil- and MS-cooled HXs)
  - Side length: 0.93-1.03 m (~3 times larger than oil- and MS-cooled HXs)
  - Pumping power: 133-140 W (~1-3 W for oil and MS)
- Average heat transfer coefficients for each fluid over various HX lengths
  - CO_2: 4310-4350 W/m^2-K
  - Oil: 517-524 W/m^2-K
  - MS: 1817-1823 W/m^2-K
  - Air: 157.5-161.3 W/m^2-K

Conclusions

- Investigated performance of PCHE as heat sink for high-temperature CO_2 HP
- Considered different sink fluids and variations in channel diameter
- Geometry
  - Optimal case aligned across fluids (1.5/1.7)
  - Marginal enhancements in power density and large increases in pressure drops with smaller channel diameters (larger channel diameters not possible with plate thickness selected)
- Sink fluids
  - Air
    - 8 x or 5 x size of MS- or oil-cooled HXs, respectively
    - Pumping power still 2 orders of magnitude larger
    - =>Hybrid design needed for feasibility with larger air-side flow passages
  - MS
    - Most compact HX
    - Higher CO_2 outlet temperature, corrosiveness, cost
    - Widely implemented with CO_2 applications (e.g., in CSP)
  - Oil
    - Reasonably compact (a little under 2 x size of MS-cooled HX)
    - Fire safety, cost
    - Less explored
- Future work: PCHE design to be developed and tested as part of a HTHP for the COMHPTES project, with thermal oil as the sink fluid

COMHPTES

Compact Heat Pump and Thermal Energy Storage System for Industrial Applications

Project Consortium

KTH VETENSKAP OCH KONST · SynchroStor · ABSOLICON · MG Sustainable · BUILD TO ZERO

Validating a CO_2-based high-temperature heat pump at KTH's Division of Heat and Power Lab

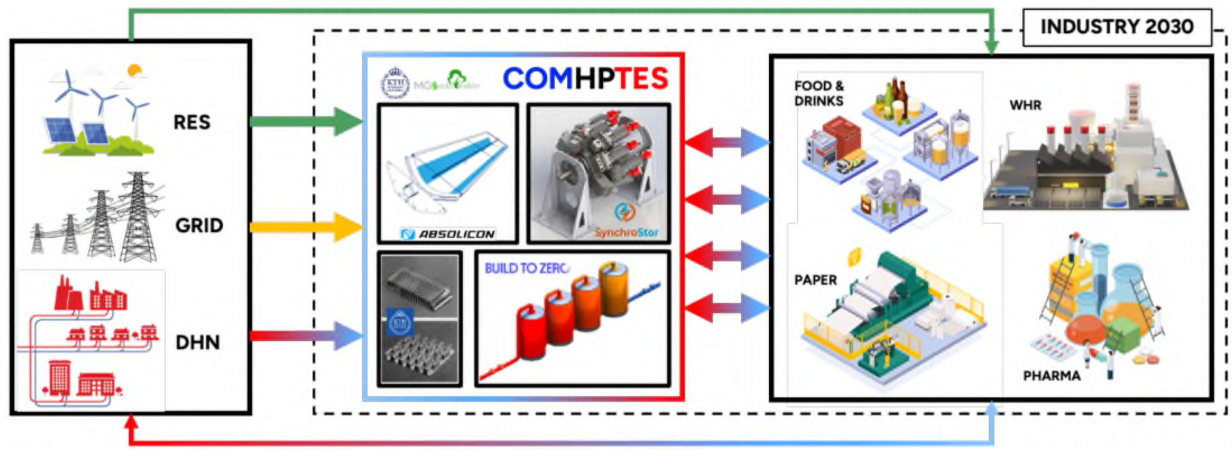

Key Facts

Providing heating and cooling

- Heating up to 325 °C
- Cooling at 5 °C

Testing real industrial use cases

Co-funded by the European Union · CETPartnership · Swedish Energy Agency · Scottish Enterprise · CDTI

Acknowledgements

This research was funded by CETPartnership, the Clean Energy Transition Partnership under the 2023 joint call for research proposals, co-funded by the European Commission (GA N°101069750) and with the funding organizations detailed on https://cetpartnership.eu/funding-agencies-and-call-modules. The project has received support from the Swedish Energy Agency, Scottish Enterprise, and the CDTI.

References

[1] Chai, L., & Tassou, S. A. (2023). Recent Progress on High Temperature and High Pressure Heat Exchangers for Supercritical CO2 Power Generation and Conversion Systems. *Heat Transfer Engineering*, *44*(21–22), 1950–1968. https://doi.org/10.1080/01457632.2022.2164683.

[2] Le Pierres, R., Southall, D., & Osborne, S. (2011). Impact of Mechanical Design Issues on Printed Circuit Heat Exchangers. *Proceedings of the SCO2 Power Cycle Symposium*, Boulder, CO, USA.

[3] Kwon, J. S., Son, S., Heo, J. Y., & Lee, J. I. (2020). Compact heat exchangers for supercritical CO2 power cycle application. *Energy Conversion and Management, 209*. https://doi.org/10.1016/j.enconman.2020.112666.

[4] Moisseytsev, A., & Sienicki, J. J. (2014). Investigation of Dry Air Cooling Option for an s-CO2 Cycle. *Proceedings of the SCO2 Power Cycle Symposium*, Pittsburgh, PA, USA.

[5] Shi, H.-Y., Li, M.-J., Wang, W.-Q., Qiu, Y., & Tao, W.-Q. (2020). Heat transfer and friction of molten salt and supercritical CO2 flowing in an airfoil channel of a printed circuit heat exchanger. *International Journal of Heat and Mass Transfer, 150*. https://doi.org/10.1016/j.ijheatmasstransfer.2019.119006.

[6] Zhu, Q., Tan, X., Barari, B., Caccia, M., Strayer, A. R., Pishahang, M., Sandhage, K. H., & Henry, A. (2021). Design of a 2 MW ZrC/W-based molten-salt-to-sCO2 PCHE for concentrated solar power. *Applied Energy, 300*. https://doi.org/10.1016/j.apenergy.2021.117313.

[7] Duratherm. *Duratherm 600 Technical Data Sheet*. Retrieved September 18, 2025 from https://durathermfluids.com/pdf/productdata/heattransfer/duratherm-600.pdf.

[8] Parida, D. R., & Basu, S. (2023). On the specific heat capacity of HITEC-salt nanocomposites for concentrated solar power applications. *RSC Advances, 13*, 5496-5508. https://doi.org/10.1039/D2RA07384F.

[9] Coastal Chemical Co., L.L.C. HITEC Heat Transfer Salt. Retrieved on September 18, 2025 from http://www.coal2nuclear.com/MSR%20-%20HITEC%20Heat%20Transfer%20Salt.pdf.

[10] Lemmon, E.W., Jacobsen, R.T., Penoncello, S.G., & Friend, D. (2000). Thermodynamic Properties of Air and Mixtures of Nitrogen, Argon, and Oxygen from 60 to 2000K at Pressures to 2000 MPa. *Journal of Physical and Chemical Reference Data, 29*(3).

[11] Span, R., & Wagner W. (1996). A New Equation of State for Carbon Dioxide Covering the Fluid Region from the Triple-Point Temperature to 1100 K at Pressures up to 800 MPa. *Journal of Physical and Chemical Reference Data, 25*(6).

[12] Jung, C., & Spenke, C. (2023). Volumetric Determination of Densities of Molten Salts for CSP Applications*. Proceedings of SolarPACES 2023, the 29th International Conference on Concentrating Solar Power, Thermal, and Chemical Energy Systems,* Sydney, Australia. https://doi.org/10.52825/solarpaces.v2i.914.

[13] Xiao, X., Zhang, G., Ding, Y., & Wen, D. (2019). Rheological Characteristics of Molten Salt Seeded with Al2O3 Nanopowder and Graphene for Concentrated Solar Power. *Energies, 12*(3), 467. https://doi.org/10.3390/en12030467.

[14] Wu, Y.-T., Chen, C., Liu, B., & Ma, C.-F. (2012). Investigation on forced convective heat transfer of molten salts in circular tubes. *International Communications in Heat and Mass Transfer, 39*(10), 1550-1555. https://doi.org/10.1016/j.icheatmasstransfer.2012.09.002.

[15] American Society of Mechanical Engineers. (2023). *2023 ASME Boiler and Pressure Vessel Code, Section VIII, Division 1*. American Society of Mechanical Engineers (ASME).

[16] American Society of Mechanical Engineers. (2023). 2023 *ASME Boiler and Pressure Vessel Code, Section II - Materials*. American Society of Mechanical Engineers (ASME).

[17] Saeed, M., Berrouk, A. S., Siddiqui, M. S., Awais, A. A. (2020). Numerical investigation of thermal and hydraulic characteristics of sCO2-water printed circuit heat exchangers with zigzag channels. *Energy Conversion and Management, 224*. https://doi.org/10.1016/j.enconman.2020.113375.

[18] Zilio, G., Moura, M.R., dos Santos, F.J., Possamai, T.S., & Mortean, M.V.V. (2024). Nusselt number analysis of printed circuit heat exchangers with straight and zigzag channels. *International Journal of Heat and Fluid Flow, 107*. https://doi.org/10.1016/j.ijheatfluidflow.2024.109395.

[19] Hesselgreaves, J. E. (2001). *Compact Heat Exchangers: Selection, Design and Operation*. Elsevier.

[20] Nellis, G. F., & Klein, S. A. (2009). *Heat transfer*. Cambridge University Press.

[21] Sullivan, S. D., Farias, J., Kesseli, J., & Nash, J. Mechanical Design and Validation Testing for a High-Performance Supercritical Carbon Dioxide Heat Exchanger. *Proceedings of the ASME Turbo Expo 2017: Turbomachinery Technical Conference and Exposition. Volume 9: Oil and Gas Applications; Supercritical CO2 Power Cycles; Wind Energy*, Charlotte, North Carolina, USA. June 26–30, 2017. V009T38A012. ASME, https://doi.org/10.1115/GT2017-63639.